

# Effect of Eccentricity on Conjugate Natural Convection in Vertical Eccentric Annuli

A. Jamal, M. A. I. El-Shaarawi, and E. M. A. Mokheimer

**Abstract**—Combined conduction-free convection heat transfer in vertical eccentric annuli is numerically investigated using a finite-difference technique. Numerical results, representing the heat transfer parameters such as annulus walls temperature, heat flux, and heat absorbed in the developing region of the annulus, are presented for a Newtonian fluid of Prandtl number 0.7, fluid-annulus radius ratio 0.5, solid-fluid thermal conductivity ratio 10, inner and outer wall dimensionless thicknesses 0.1 and 0.2, respectively, and dimensionless eccentricities 0.1, 0.3, 0.5, and 0.7. The annulus walls are subjected to thermal boundary conditions, which are obtained by heating one wall isothermally whereas keeping the other wall at inlet fluid temperature. In the present paper, the annulus heights required to achieve thermal full development for prescribed eccentricities are obtained. Furthermore, the variation in the height of thermal full development as function of the geometrical parameter, i.e., eccentricity is also investigated.

**Keywords**—Conjugate natural convection, eccentricity, heat transfer, vertical eccentric annuli.

## I. INTRODUCTION

THE study of combined conduction-natural convection heat transfer in vertical eccentric annuli is of great importance because of its many engineering applications in electrical, nuclear, solar and thermal storage fields. A typical application is that of the drilling operations of oil and gas wells. During drilling operations liquid mud is pumped from a surface mud tank via the drill pipe (several kilometers in length), through nozzles in the rotating drill bit, and back to the mud tank through the annular space between the well bore wall and the drill pipe. Natural convection may occur during idle periods and it can contribute to passive cooling of the drill pipe.

In spite of many studies in the literature for the conventional case of either forced or free convection in the developing region of eccentric annuli [1]-[11], there are few research papers available for the conjugate case in vertical eccentric annuli. The first is that of El-Shaarawi and Haider [12] for the forced convection case. They presented forced convection results for a fluid of Prandtl number 0.7 flowing in a fluid annulus of radius ratio 0.5 with eccentricities 0.1, 0.3, 0.5 and 0.7. Second and third papers by El-Shaarawi et al. [13], [14] investigated the conjugate and geometry effects on

steady laminar natural/free convection in open-ended vertical eccentric annuli, respectively. Fourth paper by Jamal et al. [15] studied the effects of geometrical parameters, such as eccentricity and annulus radius ratio, on very practical parameters known as critical conductivity ratio above which and wall thickness below which the conjugate effect can be neglected.

The literature survey summarized above revealed that many other important aspects of thermally developing conjugate natural convection heat transfer such as effect of eccentricity need to be investigated. The present paper presents a boundary-layer model for the problem of developing steady laminar conjugate natural convection heat transfer in vertical eccentric annuli. A numerical algorithm, employing finite-difference technique, is developed to solve the obtained model. Numerical results are presented to show the variation of the geometrical parameter, i.e., eccentricity ( $E$ ) affecting the height of thermal full development and heat transfer parameters such as annulus walls temperature, heat flux, and heat absorbed in the developing region of the eccentric annulus. The annulus walls are subjected to thermal boundary conditions of first kind [16], which are obtained by heating one wall isothermally whereas keeping the other wall at inlet fluid temperature.

## II. PROBLEM FORMULATION

The vertical eccentric annulus of finite height and thickness, as shown in Fig. 1, is open at both ends and is immersed in a stagnant Newtonian fluid maintained at constant temperature ( $T_o$ ). Free convection flow is induced inside this annular channel as a result of heating one of the channel walls isothermally while keeping the other wall at inlet fluid temperature, commonly known as boundary condition of first kind. It is evident from Fig. 1 that the eccentric annular geometry is symmetric about line AB, therefore, only the half symmetric section is taken for the analysis.

The flow is steady, laminar, enters the eccentric annulus with a uniform velocity distribution ( $U_o$ ). Body forces in other than the vertical direction, viscous dissipation ( $\Phi$ ), internal heat generation ( $Q'''$ ) and radiation heat transfer are absent. The governing equations describing flow and heat transfer through the eccentric annulus are the conservation equations of mass, momentum and energy given in a general orthogonal curvilinear coordinate system by Hughes and Gaylord [17].

A. Jamal is with the Mechanical Engineering Department, McGill University, Montreal, QC H3A 0G4 Canada (phone: 514-576-6860; e-mail: ahmad.jamal@mail.mcgill.ca).

M. A. I. El-Shaarawi and E. M. A. Mokheimer are with the Mechanical Engineering Department, King Fahd University of Petroleum and Minerals, Dhahran, 31261, KSA (e-mail: magedas@kfupm.edu.sa, esmailm@kfupm.edu.sa).

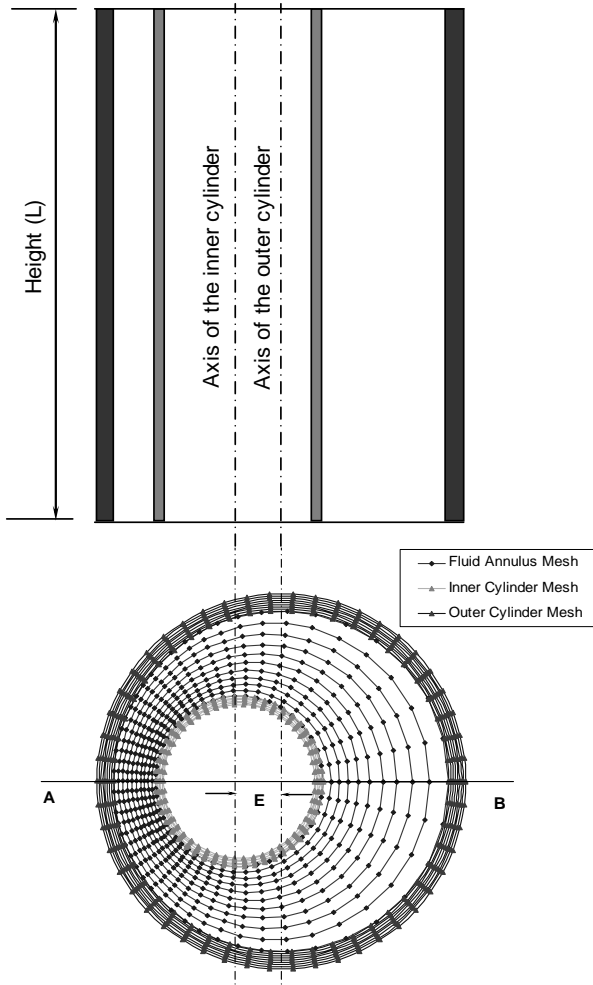


Fig. 1 The geometry and grid points

The bipolar coordinate system is more suitable to express the partial differential equations describing the flow and heat transfer through the vertical eccentric annulus, shown in Fig. 1. On the other hand, the cylinder walls have uniform thickness. Hence, the cylindrical coordinate system is more appropriate for the solid walls. Some parabolic-flow assumptions by El-Shaarawi and Mokheimer [4] will be used to simplify the governing equations. The assumptions include: the pressure is a function of the axial coordinate only ( $\frac{\partial p}{\partial \eta} = \frac{\partial p}{\partial \xi} = 0$ ), the axial diffusions of momentum and energy

are neglected ( $\frac{\partial^2}{\partial z^2} = 0$ ), and the  $\eta$ -velocity component ( $v$ ) is much smaller than  $\xi$  and  $z$ -velocity components ( $w$  and  $u$ ). Here,  $\eta$  and  $\xi$  are the first and second transverse bipolar coordinates, respectively, and  $z$  is the axial coordinate in both the Cartesian and bipolar coordinate systems. Introducing the

dimensionless parameters given in the nomenclature, carrying out the order of magnitude analysis and taking into consideration that the latter assumption results in dropping the  $\eta$ -momentum equation, the governing equations are:

A. Continuity Equation

$$\frac{\partial(HW)}{\partial \xi} + \frac{\partial(HV)}{\partial \eta} + 4(1 - NR_2)^2 \frac{\partial(UH^2)}{\partial Z} = 0 \quad (1)$$

B. Momentum Equation in Z-Direction

$$\frac{W}{H} \frac{\partial U}{\partial \xi} + \frac{V}{H} \frac{\partial U}{\partial \eta} + 4(1 - NR_2)^2 U \frac{\partial U}{\partial Z} = \frac{\theta}{4(1 - NR_2)^2} - \frac{1}{4(1 - NR_2)^2} \frac{\partial P}{\partial Z} + \frac{1}{H^2} \left( \frac{\partial^2 U}{\partial \eta^2} + \frac{\partial^2 U}{\partial \xi^2} \right) \quad (2)$$

C. Momentum Equation in  $\xi$ -Direction

$$\frac{W}{H} \frac{\partial W}{\partial \xi} + \frac{V}{H^2} \frac{\partial(HW)}{\partial \eta} + 4(1 - NR_2)^2 U \frac{\partial W}{\partial Z} - \frac{V^2}{H^2} \frac{\partial H}{\partial \xi} = \frac{1}{H^3} \left[ \frac{\partial^2(HW)}{\partial \eta^2} + \frac{\partial^2(HW)}{\partial \xi^2} \right] - \frac{2}{H^4} \left[ \frac{\partial(HW)}{\partial \eta} - \frac{\partial(HV)}{\partial \xi} \right] + \frac{\partial H}{\partial \eta} + \frac{8(1 - NR_2)^2}{H^2} \frac{\partial H}{\partial \xi} \frac{\partial U}{\partial Z} \quad (3)$$

D. Energy Equation for Fluid

$$\frac{W}{H} \frac{\partial \theta}{\partial \xi} + \frac{V}{H} \frac{\partial \theta}{\partial \eta} + 4(1 - NR_2)^2 U \frac{\partial \theta}{\partial Z} = \frac{1}{Pr H^2} \left( \frac{\partial^2 \theta}{\partial \eta^2} + \frac{\partial^2 \theta}{\partial \xi^2} \right) \quad (4)$$

E. Energy Equation for Solid

$$\frac{\partial^2 \theta_s}{\partial R^2} + \frac{1}{R} \frac{\partial \theta_s}{\partial R} + \frac{1}{R^2} \frac{\partial^2 \theta_s}{\partial \phi^2} = 0 \quad (5)$$

where,  $H$  is the dimensionless coordinate transformation scale factor,  $NR_2$  is the ratio between outer radius of inner cylinder and inner radius of outer cylinder,  $W$  is the dimensionless  $\xi$ -velocity component,  $V$  is the dimensionless  $\eta$ -velocity component,  $U$  is the dimensionless axial velocity at any point,  $P$  is the dimensionless pressure defect of fluid inside the channel at any cross section,  $\theta_s$  is the dimensionless cylinder wall temperature,  $R$  is the dimensionless radial coordinate, and  $\phi$  is the dimensionless circumferential coordinate. The thermal boundary conditions considered in this investigation are:

For outer cylinder,  $\theta_s = \theta_{s_o}$  &  $R$  vary from  $NR_3=1$  to  $NR_4$   
 For inner cylinder,  $\theta_s = \theta_{s_i}$  &  $R$  vary from  $NR_1$  to  $NR_2$

where,  $\theta_{s_o}$  is the dimensionless outer cylinder wall temperature,  $\theta_{s_i}$  is the dimensionless inner cylinder wall temperature,  $NR_3$  is the dimensionless inner radius of outer cylinder,  $NR_4$  is the ratio between outer radius of outer cylinder and inner radius of outer cylinder, and  $NR_1$  is the ratio between inner radius of inner cylinder and inner radius of outer cylinder.

#### F. Integral Form of Continuity Equation

$$\bar{U} = \frac{8(1 - NR_2)}{\pi(1 + NR_2)} \int_0^{\pi} \int_{\eta_o}^{\eta_i} UH^2 d\eta d\xi \quad (6)$$

where,  $\bar{U}$  is the dimensionless mean axial velocity,  $\eta_i$  is the first transverse bipolar coordinate at the inner wall, and  $\eta_o$  is the first transverse bipolar coordinate at the outer wall. Having the governing equations for the fluid in bipolar coordinates and the energy equations for the solid walls in cylindrical coordinates generates unmatched grid points on both the interfaces. Therefore, these points are linked to determine the temperatures at the two interfaces by applying the principles of continuity of temperature and continuity of heat flux at these interfaces. Equations (1)-(6), subject to boundary conditions of first kind, have been numerically solved as indicated in [14].

### III. NUMERICAL MODEL

Numerical results have been obtained under thermal boundary conditions of first kind for dimensionless eccentricities,  $E=0.1, 0.3, 0.5,$  and  $0.7$  at given annulus radius ratio,  $NR_2=0.5$ , solid-fluid thermal conductivity ratio,  $KR=10$ , cylinder wall thicknesses,  $\delta_i$  and  $\delta_o = 0.1$  and  $0.2$ , and Prandtl number,  $Pr=0.7$ .

In the present analysis, a grid of 25 segments in each  $\eta$  and  $\xi$  directions in the fluid annulus whereas 20 and 10 segments in the  $r$ -direction in the outer and inner cylinder walls, respectively, and 25 segments in  $\phi$ -direction in each of the cylinder walls are used [18].

### IV. VALIDATION OF NUMERICAL MODEL

To check the adequacy of the present computer code, special runs were carried out simulating the two different limiting cases of conventional and conjugate convection for the given eccentric annuli. The results of these special computer code experimentations are as follows.

First, a graphical comparison was obtained for the axial development of the mean bulk temperature,  $\theta_m$  at different eccentricities for the conventional forced convection as shown in Fig. 2. The maximum percentage difference was found to be 0.032 % depicting that the results obtained by the present computer code are in excellent agreement with that of El-

Shaarawi et al. [3].

Secondly, the present computer code was validated for the conjugate forced convection case in eccentric annuli by comparing the results obtained from a pertaining special run with the corresponding developing and fully developed temperature profiles across the widest gap ( $\psi=0$ ) of El-Shaarawi and Haider [12]; excellent agreement was observed as the maximum deviation between the obtained results and those of [12] never exceeded 0.23%. Here,  $\psi$  is the normalized value of  $\xi$ .

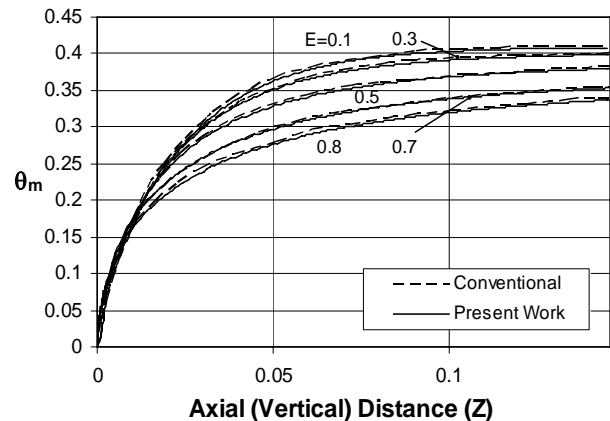


Fig. 2 Comparison of results for conventional forced convection obtained from present computer code and previously reported work [3] for mean bulk temperature against  $Z$  at various values of eccentricity

### V. RESULTS AND DISCUSSION

Fig. 3 presents the important variation of induced flow rate ( $F$ ) with the channel height ( $L$ ) for different values of the eccentricity ( $E$ ). For a given radius ratio ( $NR_2$ ), conductivity ratio ( $KR$ ) and channel height, increasing the eccentricity increases the induced flow rate. A large value of eccentricity increases the velocity asymmetry, which causes the resistance of flow to increase/decrease on the narrowest ( $\psi=1$ )/widest ( $\psi=0$ ) gap side of the annulus. The axial velocity profile develops with increasing/decreasing values on the widest ( $\psi=0$ )/narrowest ( $\psi=1$ ) gap side of the annulus resulting in a net increase in average velocity and a higher heat transfer coefficient. Consequently the mean bulk temperature increases leading to an increase in  $F$ . However, for very short channels, a reverse trend occurs, i.e., increasing the eccentricity decreases the induced flow rate. The reason is that for short channels with a large eccentricity, the axial velocity and temperature profiles do not develop sufficiently. This consequently reduces the mean bulk temperature (i.e., reduction of the buoyancy forces) and the induced flow rate.

Figs. 4 (a) and (b) represents the circumferential variation of temperatures on inner and outer solid-fluid interfaces ( $\theta_i$  and  $\theta_o$ ) at an axial (vertical) location ( $Z$ ) of  $1.99 \times 10^{-3}$  at different values of  $E$ . Small value of  $E$  shows little non-uniformity in the interface temperatures along the

circumference. The increase of  $E$  causes the temperature level to decrease on the inner solid-fluid interface at the narrowest gap ( $\psi=1$ ) and increase on the outer interface at the same gap, as can be seen in Figs. 4 (a) and (b) thus causing the non-uniformity of  $\theta_i$  and  $\theta_o$  on the interfaces to enhance.

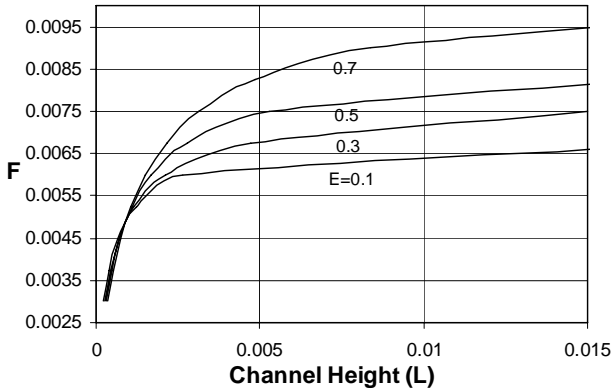
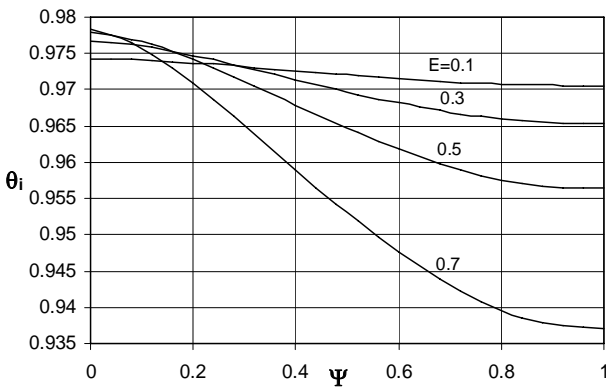


Fig. 3 Variation of flow rate with channel height for different values of eccentricity



(a) Variation of  $\theta_i$  at an axial (vertical) location of  $1.99 \times 10^{-3}$  at different values of eccentricity

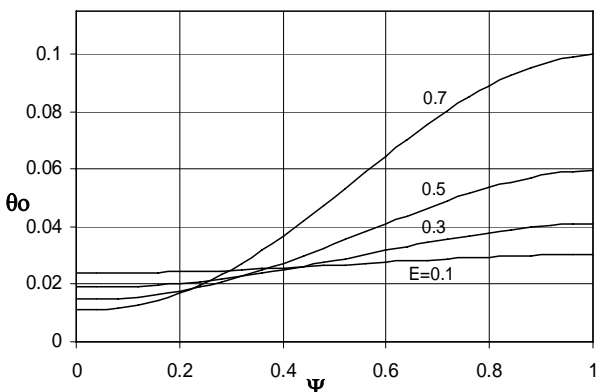
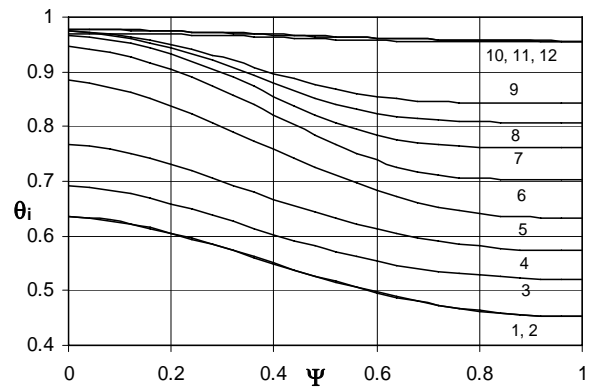


Fig. 4 (b) Variation of  $\theta_o$  at an axial (vertical) location of  $1.99 \times 10^{-3}$  at different values of eccentricity

Figs. 5 (a) and (b) present the development of circumferential temperature profiles along  $Z$  on the inner and

outer interfaces, respectively for a specific dimensionless induced flow rate,  $F=0.00675$  and  $E=0.5$ . One can clearly see that the inner interface circumferential temperature profile becomes stable earlier ( $Z=4.16 \times 10^{-4}$ ) than the outer interface temperature profile ( $Z=1.37 \times 10^{-3}$ ). Figs. 6 (a) and (b) show the effect of eccentricity on average heat flux on inner and outer solid-fluid interfaces ( $AVHF_i$  and  $AVHF_o$ ), respectively. It is observed that increasing  $E$  raises the average heat flux on both interfaces. The negative sign of  $AVHF_o$  is due to sign convention. It is also noticeable that the values of  $AVHF_i$  and  $AVHF_o$  decay and elevate sharply, respectively, close to the channel exit until these become stable after certain distance indicating that fully developed conditions have been reached.



(a) Development of  $\theta_i$  along the annulus channel axial (vertical) locations (1)  $1.000 \times 10^{-10}$  (2)  $4.251 \times 10^{-9}$  (3)  $2.291 \times 10^{-7}$  (4)  $5.479 \times 10^{-7}$  (5)  $1.191 \times 10^{-6}$  (6)  $2.411 \times 10^{-6}$  (7)  $4.622 \times 10^{-6}$  (8)  $8.478 \times 10^{-6}$  (9)  $1.499 \times 10^{-5}$  (10)  $4.157 \times 10^{-4}$  (11)  $1.366 \times 10^{-3}$  (12)  $2.863 \times 10^{-3}$

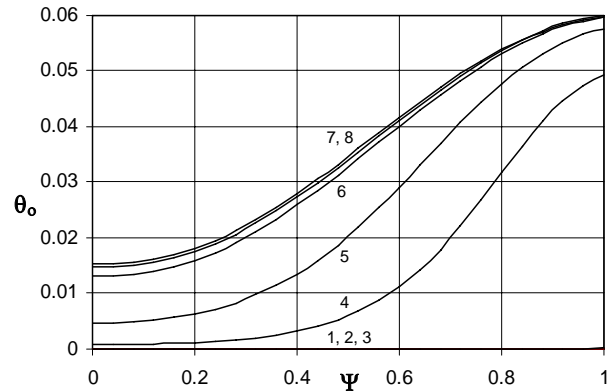


Fig. 5 (b) Development of  $\theta_o$  along the annulus channel axial (vertical) locations (1)  $1.000 \times 10^{-10}$  (2)  $5.479 \times 10^{-7}$  (3)  $1.499 \times 10^{-5}$  (4)  $1.764 \times 10^{-4}$  (5)  $4.157 \times 10^{-4}$  (6)  $1.366 \times 10^{-3}$  (7)  $1.988 \times 10^{-3}$  (8)  $2.863 \times 10^{-3}$

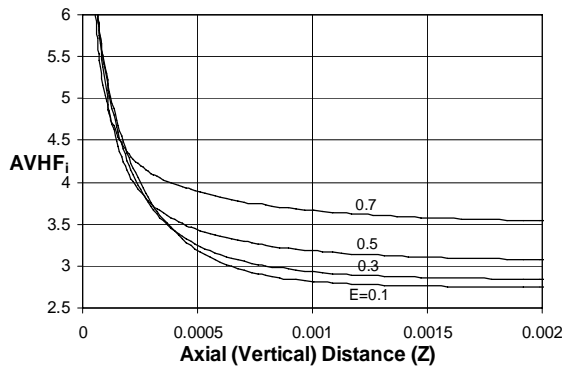


Fig. 6 (a) Axial variation of  $AVHF_i$  at different values of eccentricity

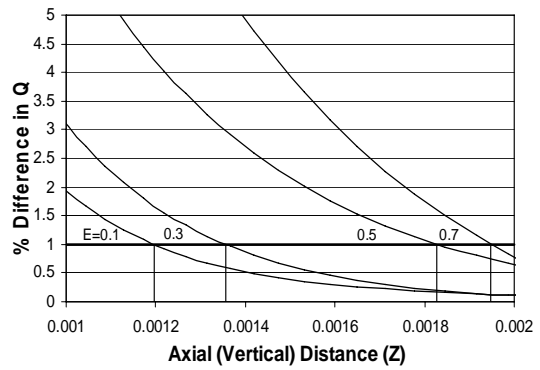


Fig. 7 Annulus axial heights required for thermal full development at different values of eccentricity

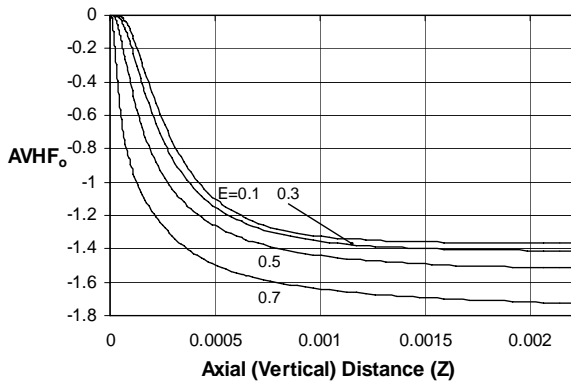


Fig. 6 (b) Axial variation of  $AVHF_o$  at different values of eccentricity

The height needed to achieve full development has been arbitrary defined as that height at which the heat absorbed by the fluid ( $Q$ ) differs by no more than 1% from the corresponding value of heat absorbed at channel exit. According to this definition, the heights for full development at different eccentricities, presented in Fig. 7, are also given in Table I for a specific induced flow rate,  $F=0.00675$ . It is obvious from the figure that higher the values of  $E$ , greater the height required for full development. In this connection, the total heat gained ( $\bar{Q}$ ) by the annulus fluid versus channel height ( $L$ ) at different values of  $E$  is also investigated and presented in Fig. 8. It is observed from the figure that for a given channel height, the amount of  $\bar{Q}$  continues to increase with  $E$ .

E	0.1	0.3	0.5	0.7
Height required to achieve thermal full development	$1.2 \times 10^{-3}$	$1.4 \times 10^{-3}$	$1.8 \times 10^{-3}$	$1.9 \times 10^{-3}$
Heat absorbed corresponding to full development height	$2.85 \times 10^{-3}$	$2.81 \times 10^{-3}$	$2.76 \times 10^{-3}$	$2.70 \times 10^{-3}$
Heat absorbed at channel exit	$2.88 \times 10^{-3}$	$2.84 \times 10^{-3}$	$2.79 \times 10^{-3}$	$2.72 \times 10^{-3}$

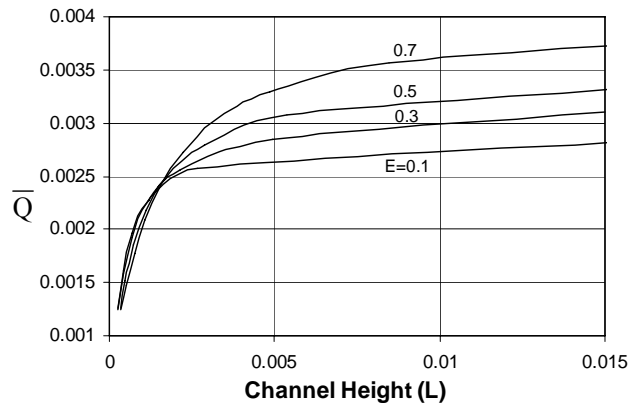


Fig. 8 Total heat absorption versus channel height at different values of eccentricity

## VI. CONCLUSION

Combined conduction-laminar free convection heat transfer in vertical eccentric annuli has been numerically investigated. A finite-difference algorithm has been developed to solve the model comprising of equations in both bipolar and cylindrical coordinate systems. Numerical results are presented for a fluid of Prandtl number,  $Pr=0.7$  in an eccentric annulus of radius ratio,  $NR_2=0.5$ . The effect of geometrical parameter, i.e., eccentricity ( $E$ ) on the variations of the induced flow rate ( $F$ ), circumferential temperatures, average heat fluxes, height for full development, and total heat absorbed ( $\bar{Q}$ ) has been investigated under thermal boundary conditions of first kind.

The results show that, for a given channel height ( $L$ ),

increasing the eccentricity causes an increase in the induced flow rate ( $F$ ). Similar trend is observed for the total heat absorbed by the fluid ( $\bar{Q}$ ) with eccentricity. Furthermore, the non-uniformity of circumferential temperature and the values of average heat flux on the interfaces increases with eccentricity. Finally, the obtained results have also shown that for a specific desired fluid suction and heat transfer with full development to achieve in the channel, higher channel must be designed, which possesses inherent larger eccentricity as compared to that having smaller eccentricity.

#### ACKNOWLEDGMENT

The support of King Fahd University of Petroleum and Minerals to carry out this investigation is gratefully acknowledged.

#### REFERENCES

- [1] E. E. Feldman, R. W. Hornbeck, and J. F. Osterle, "A numerical solution of developing temperature for laminar developing flow in eccentric annular ducts," *Int. J. Heat Mass Transfer*, vol. 25, no. 2, pp. 243-253, 1982.
- [2] A. K. Mohanty and M. R. Dubey, "Buoyancy induced flow and heat transfer through a vertical annulus," *Int. J. Heat Mass Transfer*, vol. 39, no. 10, pp. 2087-2093, 1996.
- [3] M. A. I. El-Shaarawi, H. I. Abualhamayel, and E. M. A. Mokheimer, "Developing laminar forced convection in eccentric annuli," *Heat and Mass Transfer*, vol. 33, pp. 353-362, 1998.
- [4] M. A. I. El-Shaarawi and E. M. A. Mokheimer, "Developing free convection in open-ended vertical eccentric annuli with isothermal boundaries," *Journal of Heat Transfer*, vol. 121, pp. 63-72, 1999.
- [5] E. M. A. Mokheimer and M. A. I. El-Shaarawi, "Developing mixed convection in vertical eccentric annuli," *Heat and Mass Transfer*, vol. 41, pp. 176-187, 2004.
- [6] E. M. A. Mokheimer and M. A. I. El-Shaarawi, "Maximum possible induced flow rates in open-ended vertical eccentric annuli with uniform heat flux," *International journal for Numerical Methods in Heat & Fluid Flow*, vol. 15, no. 2, pp. 161-182, 2005.
- [7] R. Hosseini, M. R. Heyrani-Nobari, and M. Hatam, "An experimental study of heat transfer in an open-ended vertical eccentric annulus with insulated and constant heat flux boundaries," *Applied Thermal Engineering*, vol. 25, pp. 1247-1257, 2005.
- [8] E. M. A. Mokheimer and S. Sami, "Conditions for pressure build-up due to buoyancy effects on forced convection in vertical eccentric annuli under thermal boundary condition of first kind," *Heat and Mass Transfer*, vol. 43, no. 2, pp. 175-189, 2006.
- [9] E. Fattahi, M. Farhadi, and K. Sedighi, "Lattice Boltzmann simulation of natural convection heat transfer in eccentric annulus," *International journal of thermal sciences*, vol. 49, pp. 2353-2362, 2010.
- [10] R. Hosseini, M. Alipour, and A. Gholaminejad, "Natural convection heat transfer of concentric/eccentric annulus subjected to inner tube of constant heat flux," in *ASME/JSME 2011 8th Thermal Engineering Joint Conference*, 2011.
- [11] F. M. Mahfouz, "Heat Convection within an eccentric annulus heated at either constant wall temperature or constant heat flux," *Journal of heat transfer*, vol. 134, no. 8, pp. 082502 (9 pages), 2012.
- [12] M. A. I. El-Shaarawi and S. A. Haider, "Critical conductivity ratio for conjugate heat transfer in eccentric annuli," *International Journal of Numerical Methods for Heat & Fluid Flow*, vol. 11, no. 3, pp. 255-277, 2001.
- [13] M. A. I. El-Shaarawi, E. M. A. Mokheimer, and A. Jamal, "Conjugate effects on steady laminar natural convection heat transfer in vertical eccentric annuli," *International Journal for Computational Methods in Engineering Science and Mechanics*, vol. 6, no. 4, pp. 235-250, 2005.
- [14] M. A. I. El-Shaarawi, E. M. A. Mokheimer, and A. Jamal, "Geometry effects on conjugate natural convection heat transfer in vertical eccentric annuli," *International Journal of Numerical Methods for Heat & Fluid Flow*, vol. 17, no. 5, pp. 461-493, 2007.

- [15] A. Jamal, M. A. I. El-Shaarawi, and E. M. A. Mokheimer, "Critical conductivity ratio and wall thickness for conjugate natural convection heat transfer in vertical eccentric annuli," *Numerical heat Transfer, Part A: Applications*, vol. 59, pp. 719-737, 2011.
- [16] W. C. Reynolds, R. E. Lundberg, and P. A. McCuen, "Heat transfer in annular passages. General formulation of the problem for arbitrary prescribed wall temperatures or heat fluxes," *Int. J. Heat Mass Transfer*, vol. 6, pp. 483-493, 1963.
- [17] W. F. Hughes and E.W. Gaylord, *Basic Equations of Engineering Science*. Schaum Outline Series, 1964, pp. 150-151.
- [18] A. Jamal, *Conjugate free convection heat transfer in vertical eccentric annuli*, MS Thesis, Mechanical Engineering Department, King Fahd University of Petroleum and Minerals (KFUPM), Dhahran, Saudi Arabia, 2002, pp. 52-57.

**A. Jamal** (B.E.'98-M.S.'2002) was born in Saudi Arabia in 1974. He obtained his Bachelor's degree in Mechanical Engineering from University of Engineering and Technology, Lahore, Pakistan in 1998. Later, he completed his Masters of Science in Mechanical Engineering from King Fahd University of Petroleum and Minerals, Dhahran Saudi Arabia in 2002. Afterwards, he joined the Aerospace Engineering Department as faculty at the same University. Now he is pursuing his PhD in Mechanical Engineering at McGill University.

He also has experience in working for Swedish multi-national company Tetra Pak as shift in charge in the Production Department. He is the author of 15 international refereed journal and conference publications, and one of the major contributors in the preparation of two lab course manuals, which are used as text material. His research interests include but not limited to heat transfer, fluid mechanics, reliability analysis, and fluid-structure interactions.

Mr. Jamal was the member of ASME and AIAA. He is the recipient of the McGill Engineering Doctoral Award (MEDA) granted by McGill University (2008-2011), Award of distinguished Services as a Coordinator for the Cooperative Program, May 19, 2004, and Aerospace Engineering Faculty Services Award, 2003-2004. He is also Included in the Marquis Who's Who in Science and Engineering, 10<sup>th</sup> Anniversary Edition.

**M. A. I. El-Shaarawi** is professor of Mechanical Engineering at King Fahd University of Petroleum and Minerals, Dhahran, Saudi Arabia. He graduated from the Mechanical Engineering Department at Cairo University in 1967 and obtained his MS degree from the Mechanical Engineering Department at Al-Azhar University in Cairo. He obtained his PHD degree from Leeds University, England in 1974.

**E. M. A. Mokheimer** Dr. Mokheimer obtained his Ph. D. degree in Mechanical Engineering from KFUPM in 1996. His research interests are in the area of computational fluid dynamics and heat transfer. Dr. Mokheimer is working as an Associate professor at KFUPM. Dr. Mokheimer has published over 65 papers in reputable refereed international journals and conferences in this area.

In his research, Dr. Mokheimer used to develop his own Computational Fluid Dynamics and Heat Transfer (CFDHT) codes using FORTRAN, MATLAB and the user friendly spreadsheet programs. Moreover, Dr. Mokheimer has experience in using commercial CFDHT codes such as FLUENT and ANSYS. Dr. Mokheimer has a good experience and background in the thermal sciences related to thermal power plants with particular interest in combustion, gas and steam turbines performance. Dr. Mokheimer has visited most of the thermal and hydraulic power plants in the Kingdom of Saudi Arabia and Egypt (including the desalination-electric) co-generation plants and in Egypt with his classes of thermal power plants course. Recently Dr. Mokheimer devoted his attention to the heat transfer applications in Power generation Plants and Air Conditioning. In this regard, Dr. Mokheimer is focusing on Energy savings aspects. Dr. Mokheimer is involved now as a principle investigator in more than one project on integrating Concentrated Solar Power Technologies with Conventional Power Plants generation and Absorption Refrigeration Technologies.